

LIST OF FIGURES

1	(a) Evolution of NMSE for each method with varying low-rank noise power with 100 Monte Carlo simulations. (b) Reconstructed images of the three methods under varying levels of low-rank noise. The low-rank noise with rank 1 is added into the observed visibility. The power of the low-rank noise is defined relative to the source power, $P_{\text{LRdB}} = 10 \log_{10}(P_{\text{LR}}/P_0)$, where $P_0 = \ \mathbf{x}\ ^2$ is the power of the true image and P_{LR} is the power of the low-rank matrix \mathbf{W}_k	2
2	(a) Evolution of NMSE of the three methods with varying RFI noise power with 100 Monte Carlo simulations. (b) Reconstructed images of the three methods under varying levels of RFI noise. To simulate RFI noise, we model 100 RFI events as additional point sources with same power into the scene. Only 20% of the visibilities are affected by the RFI, reflecting the selective impact on sensors. The power of each RFI is defined relative to the source power, $P_{\text{RFIdB}} = 10 \log_{10}(P_{\text{RFI}}/P_0)$, where P_{RFI} is the power of random point noise.	3
3	(a) Evolution of NMSE and for each method with varying RFI noise power with 100 Monte Carlo simulations. (b) Reconstructed image of the four methods under varying levels of RFI noise. To simulate RFI noise, we model 100 RFI events as additional point sources with same power into the scene. Only 20% of the visibilities are affected by the RFI, reflecting the selective impact on sensors. The power of each RFI is defined relative to the source power, $P_{\text{RFIdB}} = 10 \log_{10}(P_{\text{RFI}}/P_0)$, where P_{RFI} is the power of random point noise.	4

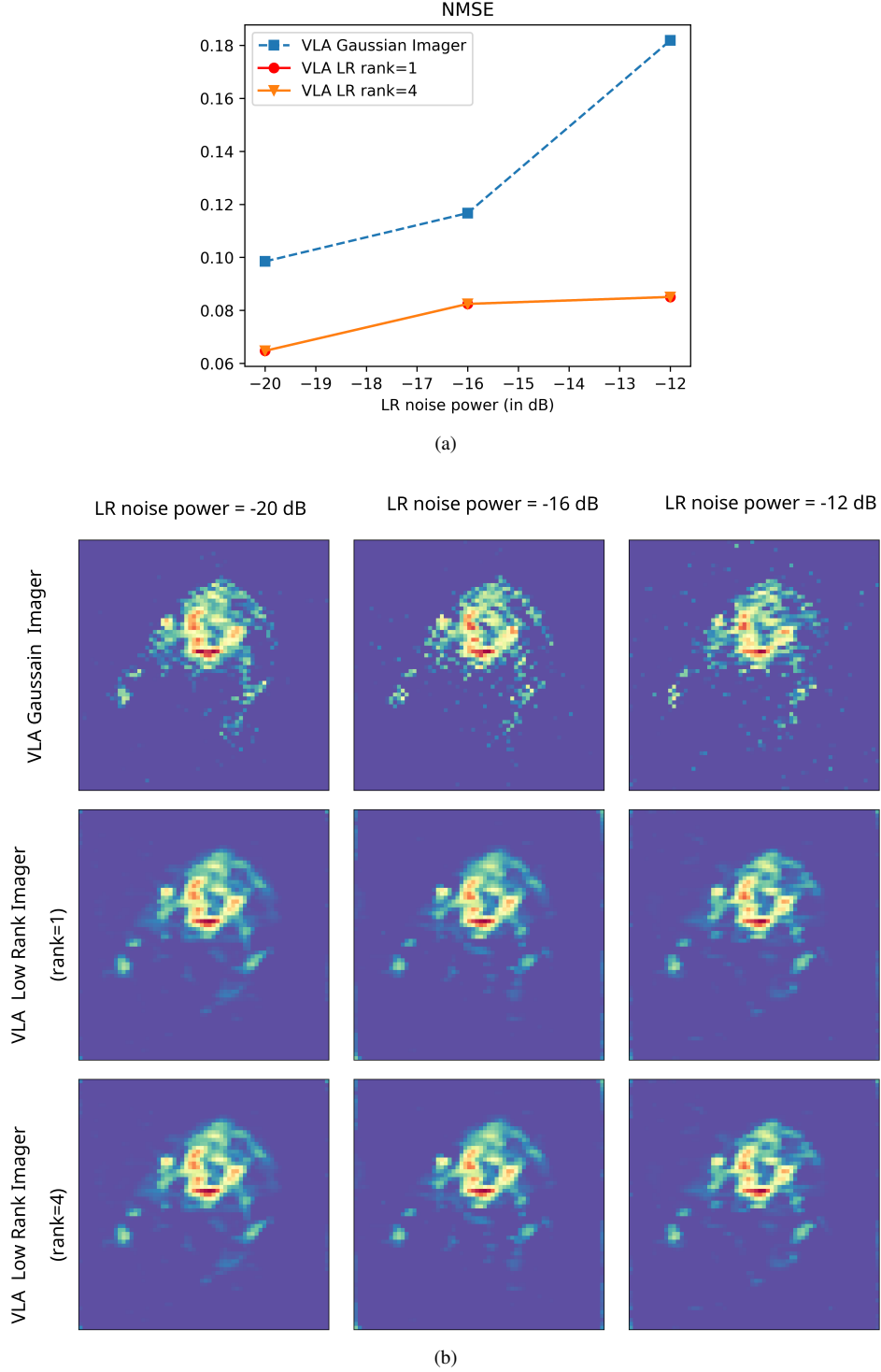


Fig. 1: (a) Evolution of NMSE for each method with varying low-rank noise power with 100 Monte Carlo simulations. (b) Reconstructed images of the three methods under varying levels of low-rank noise.

The low-rank noise with rank 1 is added into the observed visibility. The power of the low-rank noise is defined relative to the source power, $P_{\text{LRdB}} = 10 \log_{10}(P_{\text{LR}}/P_0)$, where $P_0 = \|\mathbf{x}\|^2$ is the power of the true image and P_{LR} is the power of the low-rank matrix \mathbf{W}_k .

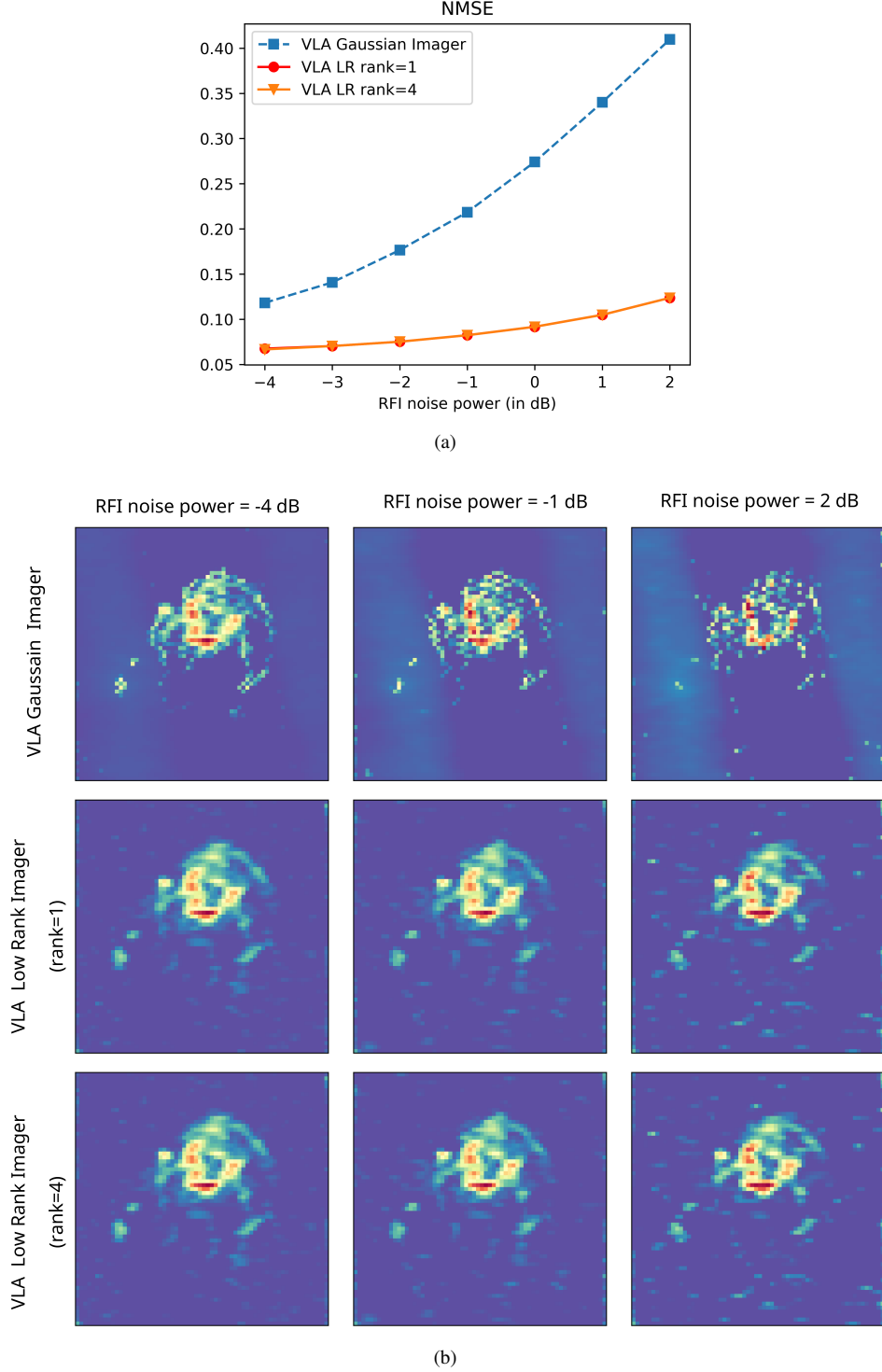


Fig. 2: (a) Evolution of NMSE of the three methods with varying RFI noise power with 100 Monte Carlo simulations. (b) Reconstructed images of the three methods under varying levels of RFI noise.

To simulate RFI noise, we model 100 RFI events as additional point sources with same power into the scene. Only 20% of the visibilities are affected by the RFI, reflecting the selective impact on sensors. The power of each RFI is defined relative to the source power, $P_{\text{RFI dB}} = 10 \log_{10}(P_{\text{RFI}}/P_0)$, where P_{RFI} is the power of random point noise.

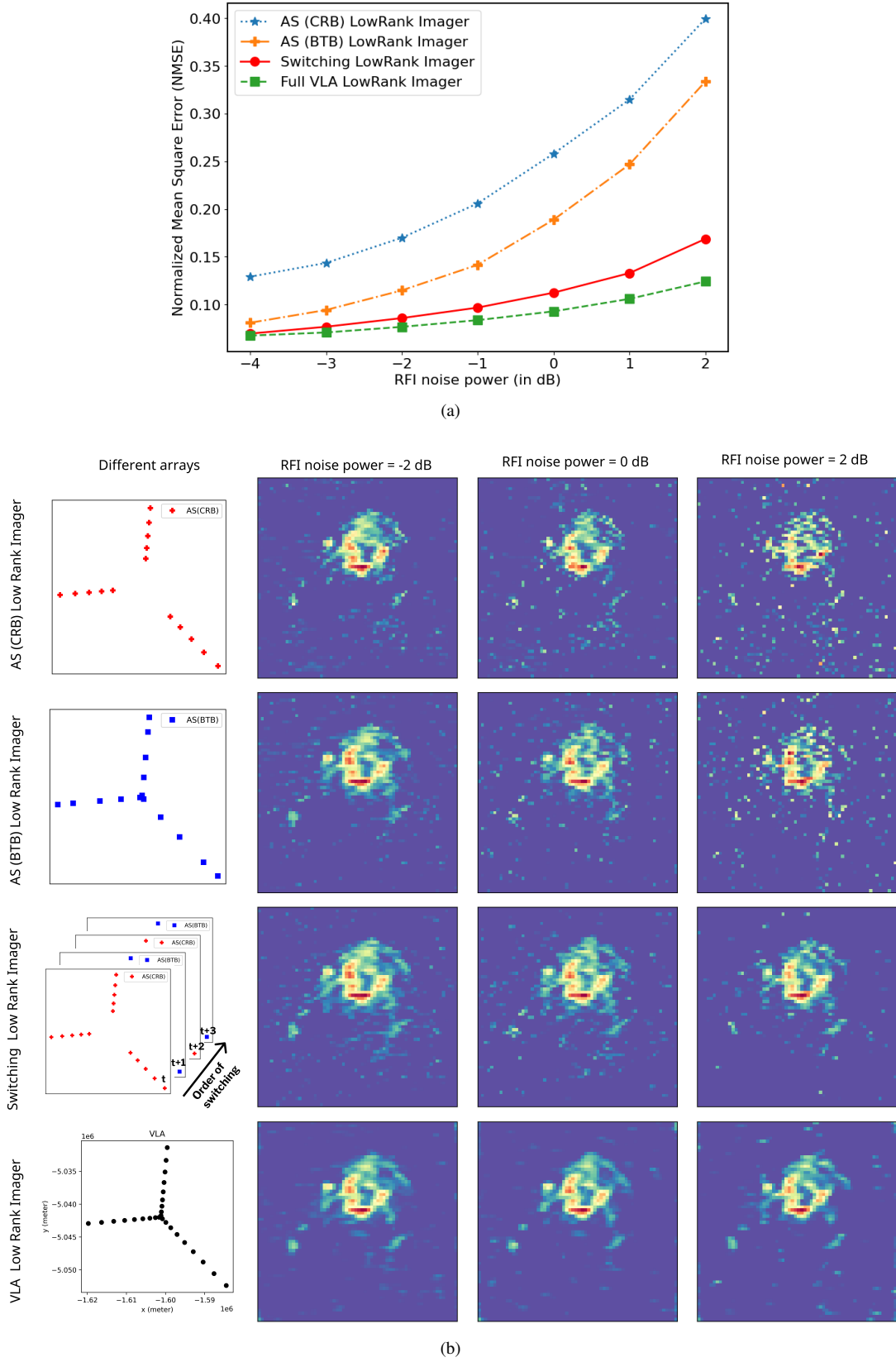


Fig. 3: (a) Evolution of NMSE and for each method with varying RFI noise power with 100 Monte Carlo simulations. (b) Reconstructed image of the four methods under varying levels of RFI noise.

To simulate RFI noise, we model 100 RFI events as additional point sources with same power into the scene. Only 20% of the visibilities are affected by the RFI, reflecting the selective impact on sensors. The power of each RFI is defined relative to the source power, $P_{\text{RFIdB}} = 10 \log_{10}(P_{\text{RFI}}/P_0)$, where P_{RFI} is the power of random point noise.